

The Physical and Engineering Requirements of Scalable, Decentralised, Distributed, Large-Scale MIMO

Gerard Borg, Zia-Ud-Din Javaid and Asaduzzaman Khandaker
Research School of Physics and Engineering ANU College of Science.
Australian National University
ACT 2601 Australia
gerard.borg@anu.edu.au

Abstract—In recent papers [1], [2] we introduced a novel approach to the deployment of wireless infrastructure by scalable, distributed, decentralised MIMO. SDD-MIMO is a novel wireless network architecture specifically intended for wireless broadband infrastructure whose aggregate capacity and range scale as service antenna nodes are added to the network. We previously considered the physical and engineering constraints of such a system [1] and produced a compelling deployment simulation of wireless broadband for an over-the-horizon transoceanic troposcatter link of 155 kms extent [2]. The key issue is how to achieve scalable broadband over a long range. In this paper we discuss the engineering and physical constraints from a practical perspective. We take a close look at how the beam-forming process works. We propose a novel definition of capacity expressed in terms of the correlation between the received and transmitted signals. We demonstrate through Monte-Carlo simulations that this capacity agrees well with that previously derived for cell-free massive MIMO [3]. Moreover, the Monte-Carlo simulation allows us to explore the fluctuations in capacity versus the size of the network. We show that the capacity per user converges to the theoretical value as the network increases in size. For the SDD-MIMO network work to function, one must also solve the problem of global synchronisation of radio carrier frequencies and information symbols. We show that a well known low-cost GPS technique may be used to achieve this goal. Finally we take a look at what is probably the main constraint of distributed MIMO: the communication of beam-forming information across the Internet back-haul. We present some preliminary results demonstrating that adequate throughputs and latencies can be expected.

Index Terms—MIMO, wireless, scalable, distributed, decentralised, Internet, broadband, regional, remote.

I. INTRODUCTION

In wireless networks distributed over large ranges such as that depicted in Fig.1 huge gains in capacity can be achieved by frequency reuse as a result of distributed beam forming [1], [2]. Under conditions of conjugate match MIMO beam-forming, net capacity scales with the number of users when their number is less than the number of base stations [3]. Coverage and range are superior to that of conventional cellular networks [2]. A scalable, distributed and decentralised, SDD-MIMO network allows the reuse of spectrum through spatial multiplexing of multiple antennas at the transmitter and the receiver. In this architecture the base stations can be distributed

over tens of kilometres. The size of the network allows for highly resolved spatial selectivity as the base stations behave as a very large antenna array. For such a network to be viable however, there are a number of physical and engineering issues that need to be resolved.

In this paper we address the following issues.

- Under what conditions can one expect the capacity per user to scale in accordance with eqn. (3) of [1]?
- How can global synchronisation of carrier frequencies and symbol times be achieved across the network?
- How well can one expect the beam-forming information to be transported across a TCP-IP back-haul network?
- Is the complexity of the channel codec achievable in low cost hardware?

We treat these issues from a practical perspective. This paper is structured as follows. In section II we discuss the beam-forming process in detail. In section III, we use these results to perform a Monte-Carlo simulation of capacity which provides some useful insights into the reliability of the network. In section IV we propose a simple technique to achieve synchronisation. In section V we present simple experiments that demonstrate the feasibility of beam-forming over a back-haul TCP-IP network. In section VI we study the channel codec and ask whether it can be achieved in low cost hardware. Finally in section VII we conclude.

II. DISTRIBUTED BEAM-FORMING

Although SDD-MIMO like all MIMO architectures, can use any number of signal processing techniques such as MMSE, Zero-forcing etc for MIMO processing, one of the most intuitive techniques to understand is conjugate match beam-forming [4]. For reasons to be explained, conjugate match beam-forming is also referred as *time reversal communications* [5] and forms the basis of the *time reversal mirror* [6]. Fig. 1 shows the layout of a large-scale SDD-MIMO network. The dark spots are the service nodes (SN) and the squares are the remote nodes (RN). The SNs perform MIMO processing by coordination over a network back-haul shown as thick lines. Usually the back-haul network is a TCP-IP network. When separate back-haul is unavailable, for example in the form of

a switch, then the Internet itself can serve as the network over which the MIMO processing is performed. We consider some performance issues later on.

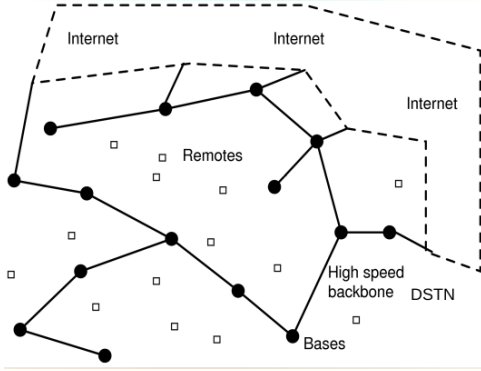


Fig. 1. General layout of a large-scale SDD-MIMO network.

A. The Time Reversal or Conjugate Match Beam-forming Process

Consider an individual SISO link between the m -th RN and the n -th SN. The complex signal received in the baseband is related to the symbols $x(t)$ transmitted by,

$$y(t) = \sum_{t'=0}^{T-1} h_{nm}(t-t')x(t') + \tilde{N}(t) \quad (1)$$

where $y(t)$ is the signal received as a function of time and $x(t)$ is the transmitted symbol. The quantity $\tilde{N}(t)$ is additive white noise AWGN. The complex number h_{nm} is the channel coefficient between the n -th SN to the m -th RN including the effects of the SN and RN electronics. In this paper we assume that the channel coefficients are gaussian distributed. The time t is considered a discrete index marking the symbol periods. The index T is the maximum time delay in the channel measured in symbol periods.

To implement distributed beam-forming over a vast network, the SNs aim to deliver maximum signal to the chosen RN by properly phasing their signals. Consider first the down-link where beam-forming must be performed prior to transmission. For the case of the ISI multipath channel of eqn. 1 the *time reversal precoded* signal for the n -th SN consists of the sum of the convolutions of the time reversed and complex conjugated channel coefficients with the symbols of each RN. We transmit symbols from the n -th SN to the μ -th RN with a weighting equal to the amplitude of the channel coefficient $h_{n\mu}^*$. This is not the only choice we could make. Similar results would be obtained if we were to choose a unity gain coefficient $h_{n\mu}^*/|h_{n\mu}|$ for example. In this analysis we divide the transmitted power from each SN by M (the number of RNs) i.e. divide the signal transmitted by \sqrt{M} . As a result, we may write the following for the signal transmitted by each SN,

$$y_n(t') = \frac{1}{\sqrt{M}} \sum_{\mu=0}^{M-1} \sum_{t''=0}^{T-1} h_{n\mu}^*(t'+t'')x_\mu(t'') \quad (2)$$

Using eqn. 1, the signal received by the m -th remote can therefore be written,

$$z_m(t) = \sum_{n=0}^{N-1} \sum_{t'=0}^{T-1} h_{nm}(t-t')y_n(t') + \tilde{N}(t) \quad (3)$$

Eqn (3) describes down-link distributed beam forming in an ISI multipath channel.

Consider the problem of supplying M RNs with independent data from N SNs as shown in Fig. 1. Due to the large interference levels on such a network, we assume that the data symbols to be transmitted use QPSK modulation. Furthermore without loss of generality, we let $T=1$ (single tap channel). This assumption is general in the event that OFDM (Orthogonal Frequency Division Multiplexing) is used. In this case eqns. (2) and (3) yield,

$$z_m(t) = \frac{1}{\sqrt{M}} \sum_{n=0}^{N-1} \sum_{\mu=0}^{M-1} h_{nm}h_{n\mu}^*x_\mu(t) + \tilde{N}(t) \quad (4)$$

From this, we can compute the “wanted” power at the m -th RN. The wanted power is that directed by all SNs toward the m -th RN in order to communicate the symbol x_m . We note that the expectation of $\langle h_{nm}h_{\nu\mu}^* \rangle = 0$ if either $m \neq \mu$ or $n \neq \nu$. In this case the wanted power P_w is given by,

$$P_w = \frac{1}{M} \left(\sum_{n=0}^{N-1} |h_{nm}|^2 \right)^2 |x_m|^2 \quad (5)$$

Similarly, the unwanted or interfering power P_u due to cochannel interference is given by,

$$P_u = \frac{1}{M} \sum_{n=0}^{N-1} \sum_{\mu \neq m}^{M-1} |h_{nm}|^2 |h_{n\mu}|^2 |x_\mu|^2 \quad (6)$$

Conjugate match beam-forming attempts to steer the signal power toward each RN. When there are many SNs and few RNs, the beams can be intense. Fig. 2 shows some computed thermal images of these beams. As the number of SNs increases, the beams become more intense as expected. However the number of beams does not increase with the number of SNs. The number of beams is determined by both the number of RNs and the dimensions of the SN network. The multiplicity of these beams is a pictorial representation of the degrees-of-freedom (DoF) available to the system. The number of DoFs is diffraction limited as already discussed in [1].

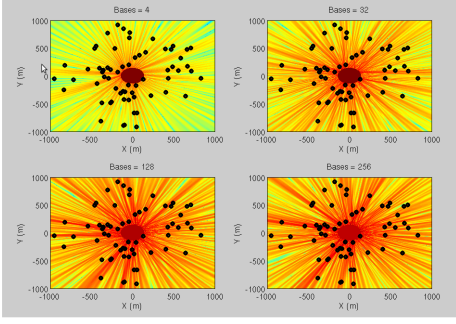


Fig. 2. Hot spot maps showing the high resolution beams of SDD-MIMO.

B. Capacity

Using the noise power, $P_N = \langle \tilde{N} \rangle^2$ and the interference power P_u , we define the signal to interference and noise ratio (SINR) = $P_w / (P_u + P_N)$. Shannon's capacity rule may therefore be written [8],

$$C = \log_2(1 + \text{SINR}) \quad (7)$$

If we set each channel power to the mean $\epsilon = |h_{nm}|^2$ over all links and noting that $P_w = N^2/M\epsilon|x_m|^2$ and $P_u = N(M-1)/M\epsilon|x_m|^2$, then we obtain the following simple formula for capacity in the limit $1 \ll M$,

$$C = \log_2 \left(1 + \frac{N^2}{M} \frac{\text{SNR}}{N \cdot \text{SNR} + 1} \right) \quad (8)$$

where SNR is the signal to noise ratio for one SN / RN. This is the same as eqn. 3 of [1] as derived on the basis of [3].

C. Range and Coverage

Apart from the obvious observation that a network of distributed SNs allows for the network to 'point around obstacles' to connect isolated RNs, the overall range of the network is also enhanced in SDD-MIMO. Instead of treating each channel coefficient to be Rayleigh distributed, we here treat the case where the SNs are localised over an area of dimension $D \gg \lambda$ and the RN are located at some range $R_{nm} \gg D$. If in addition the channel is line-of-sight then the Friis transmission model applies and the magnitude of each channel coefficient may be written,

$$|h_{nm}|^2 \approx \frac{G_T G_R \lambda^2}{(4\pi R_{nm})^2} = \left(\frac{\lambda}{4\pi R_m} \right)^2 \quad (9)$$

where G_T and G_R are the antenna gains at the SN and RN which for the sake of simplicity we take to be unity. For $D \ll R_{nm}$, $R_{nm} = R_m$ does not depend on n .

Approximately speaking, the range of the SDD-MIMO link is given by the distance at which $P_w = P_u + P_N$. To compute it we note using eqn. (9) that

$$P_w = \frac{N^2}{M} \left(\frac{|x_m| \lambda}{4\pi R_m} \right)^2, \quad P_u = \frac{N(M-1)}{M} \left(\frac{|x_m| \lambda}{4\pi R_m} \right)^2 \quad (10)$$

The range of the SDD-MIMO link is therefore given by the following expression,

$$\left(\frac{|x_m| \lambda}{4\pi R_m} \right)^2 = \frac{M P_N}{N(N-M+1)} \quad (11)$$

Similarly for a SISO link under Friis transmission the range R_S occurs when $P_r = P_N$, where

$$\left(\frac{|x_m| \lambda}{4\pi R_S} \right)^2 = P_N \quad (12)$$

Note that for a SISO link the entire SN power is dedicated to the transmission. Dividing eqns (11) and (12) we obtain,

$$\frac{R_m}{R_S} = \sqrt{\frac{N}{M(N-M+1)}} \quad (13)$$

Eqn. 13 shows that for $M \ll N$, the ratio of the range of the SDD-MIMO network to that of a single link scales as N .

D. Comparison with Simulations

In this section we compare net capacity, BER and range of the SDD-MIMO infrastructure network with the SISO infrastructure network.

1) *Net Capacity and Bit Error Rate*: Assuming a Rayleigh distributed ISI limited AWGN-free channel with $T = 50$ taps we can use eqn. (3) to compute net capacity and BER for QPSK. Fig. 3 shows the net capacity for 100 SNs as a function of the number of RNs on the network. Capacity points were computed from the simulation by independent computations of the wanted and unwanted powers. The line shows the analytical C_{net} result of eqn. (8). The effect of the multiplying factor of M is clearly evident. These results are spectacular. They indicate that over 100 RNs can be served on *exactly the same wireless spectrum*.

Further insights can be obtained by examining the Bit Error Rate (BER) for hard decision decoding of QPSK. The QPSK BER for a link limited by AWGN is given by,

$$\text{BER}_{QPSK} = \text{erfc}(\sqrt{Eb/N_0})/2; \quad (14)$$

In analogy with the AWGN case for QPSK we may write $Eb/N_0 = \text{SIR}/2$. Fig. (3) shows the BER and SIR as a function of the number of Rns for gaussian channel coefficients. The points on the BER curve are calculated from the model. The line through the points is the theoretical curve of eqn. (14). The agreement is excellent. Also shown in the figure is the SIR obtained from the simulation for reference.

From Fig. 3 shows good agreement between the analytical formulas and the model. The scaling of BER essentially mimics the same loss of performance that we are already familiar with in SISO networks with the same SNR as SINR. Fig. 3 indicates that the BER limited by SIR can be achieved by any traditional FEC scheme. Best performance of course

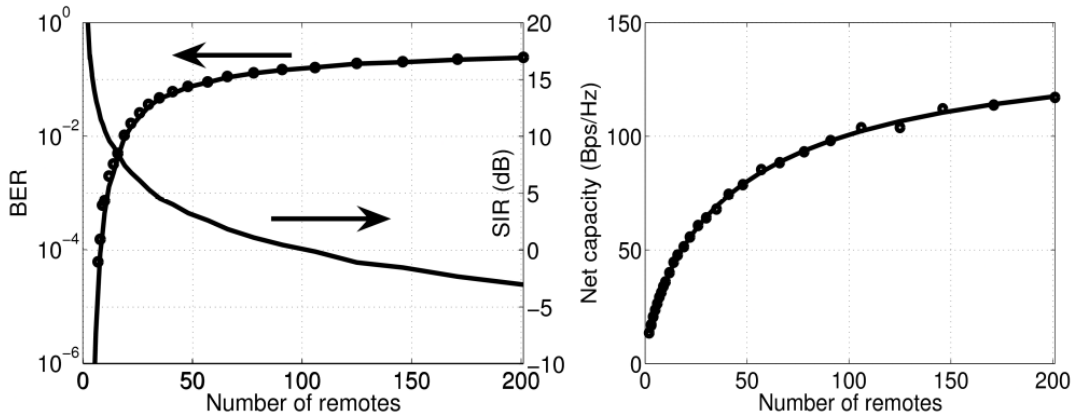


Fig. 3. The performance of the theoretical bit error rate (left) and capacity of SDD-MIMO with conjugate match beam-forming and QPSK signaling.

would be obtained by those schemes that employed advanced FEC such as iterative decoders in order to approach the performance of Fig. 3. Given that RF power and spectrum can be bought for free by the addition of extra SNs in the SDD-MIMO discussed here, it may be possible that some existing infrastructure networks (for example 802.11 WiFi) might be upgradable to a SDD-MIMO network of the kind described here using the same RNs and by replacing the APs with SDD-MIMO SNs.

III. MONTE-CARLO SIMULATIONS OF CAPACITY

Correlation between the symbols transmitted and those received can provide a measure of mutual information [7]. For a gaussian channel the mutual information is related to the correlation coefficient, ρ by

$$I(X, Y) = 0.5 \log \left(\frac{1}{1 - \rho^2} \right) \quad (15)$$

Eqn. 15 applies to a simple linear channel in which the received symbols are equal to the transmitted symbols distorted by AWGN. This is a useful formula because it allows us to deduce capacity using known transmitted data symbols from the SNs and the resultant received signals at the RN. Interestingly, such a formula is not dependent on any special considerations that might arise from the MIMO situation since in a MIMO Monte-Carlo simulation, all the symbols are taken into account at the same time.

Before we can use this formula however we need to generalise it to the case of an arbitrary channel. For simplicity we consider just the gaussian channel of section II. First consider the received signal given by eqn. 4 which can be rewritten as,

$$z_m(t) = \frac{1}{\sqrt{M}} \left(\sum_{n=0}^{N-1} |h_{nm}|^2 \right) x_m(t) + \frac{1}{\sqrt{M}} \sum_{n=0}^{N-1} \sum_{\mu \neq m} h_{n\mu} h_{nm}^* x_\mu(t) + \tilde{N}(t) \quad (16)$$

$$z_m(t) = \frac{1}{\sqrt{M}} \left(\sum_{n=0}^{N-1} |h_{nm}|^2 \right) x_m(t) + \tilde{I}(t) \quad (17)$$

where $\tilde{I}(t)$ indicates noise and interference or unwanted signals. To eliminate the channel, consider the Fourier Transforms \mathcal{L} , of received signal $z_m(t)$ and transmitted symbols $x_m(t)$, where $\mathcal{L}\{z_m\} = Z_m$ and $\mathcal{L}\{x_m\} = X_m$ and define,

$$C_{xz} = \frac{\mathcal{L}^{-1}(X_m Z_m^*)}{\sqrt{\sum |x_m|^2} \sqrt{\sum |z_m|^2}} \quad (18)$$

and hence definition of $\rho = \sqrt{\sum |C_{xz}|^2 - 1}$.

Figs. 4 and 5 show a comparison between the correlation capacity of eqn. 15 with $\rho = \sqrt{\sum |C_{xz}|^2 - 1}$ and the capacities of equations 7 and 8.

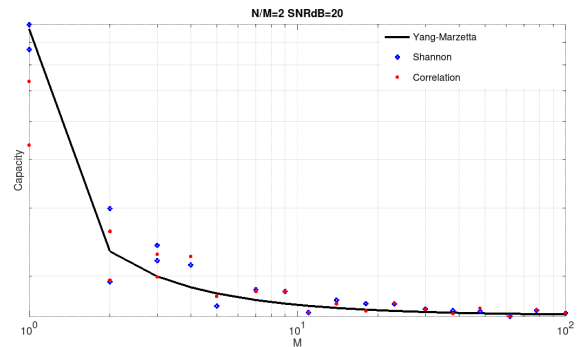


Fig. 4. Computed mean capacities per user for a SDD-MIMO network with $N = 2M$, SNR 20dB and gaussian channels.

These results show good general agreement between the various methods of calculating capacity. In particular note that the Monte-Carlo simulation in Fig. 5 suggests that the capacity per user becomes much more predictable and approaches the mean as the number of SNs and RNs increases.

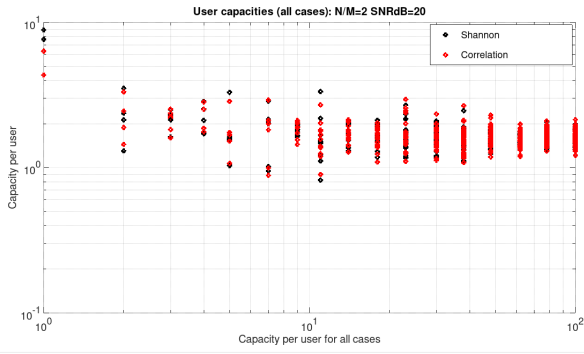


Fig. 5. Computed capacities per user for all users with $N = 2M$, SNR 20dB and gaussian channels. Here the individual user correlation capacities are shown.

IV. CARRIER AND TIMING SYNCHRONISATION

A crucial requirement of the SDD-MIMO network is that carrier local oscillators and information symbols be synchronised across the geographically distributed SN network. We demonstrate that this can be done with a common GPS that provides the 1-PPS (pulse-per second) timing signal. Such a GPS can be used to provide a GPSDO (GPS disciplined oscillator).

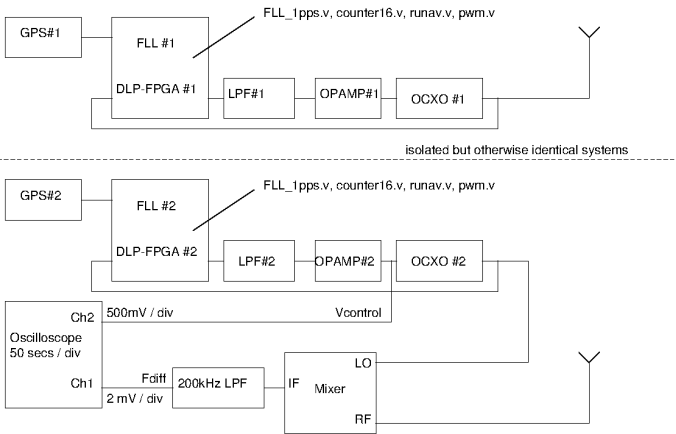


Fig. 6. Experimental setup for global carrier synchronisation test

We have demonstrated this for carriers in the sub-GHz range using the experimental setup of Fig. 6. The 1-PPSs from a pair of GPSs are inputs to a pair of FPGA development platforms located in isolated locations. Each FPGA is loaded with code that implements a frequency lock loop (FLL). The signals are transmitted through the air from a pair of antennas and mixed together by an RF mixer. The low frequency product of the mixer output provides a measure of the phase stability between the two carriers.

Results for 50MHz are shown in Fig. 7. In the top trace over the first 500 seconds, the GPSs are warming up and the FLLs converging to lock. During this time the carriers are quite different and the network inoperable. However for later times the phase offsets are quite stable even though they drift. The observed coherence time is in the order of 10 secs which

is ample to keep the carriers locked across the network for the MIMO processing to function correctly.

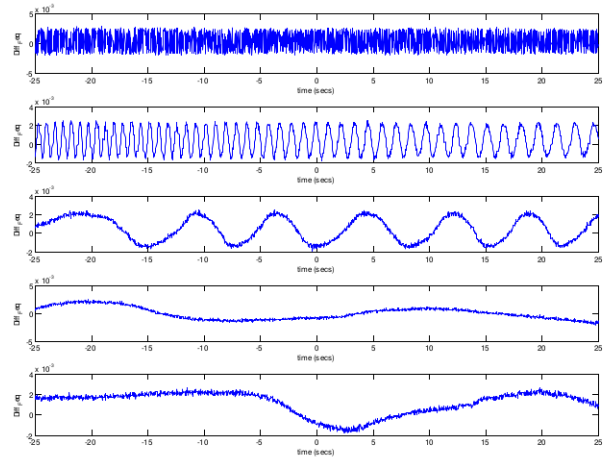


Fig. 7. Global carrier phase difference for GPS carrier lock at 50MHz

GPS timing is accurate to at least 20ns and can be constant for many seconds. This long coherence time simplifies estimation of the down-link channel because there is ample time to feed the channel estimate from RNs to the SNs over the wireless link.

V. BEAM-FORMING OVER A TCP-IP BACK-HAUL

Decentralisation of the SDD-MIMO network requires it to operate in a P2P fashion i.e. with node discovery over the Internet. This is similar to other P2P technologies such as *bittorrent* and *Hamachi Logmein*. This is currently under development and several approaches have been attempted. For the present results we used ENET as a P2P development platform¹.

The major engineering constraint however is that the communication of beam-forming information such as channel coefficients and user symbols over the back-haul is a high overhead process. For example, each SN computes the channel coefficients on the up-link and each RN on the down-link. The SN are each paired with a unique RN [4] so that signal processing can be distributed over all SNs. Equations 4 and 5 show that each SN must be in possession of all channel coefficients involving its paired RN on the up-link and the channel coefficients from the SN to each RN on the down-link. These must be communicated between SNs over the back-haul network². There are two main issues that need to be addressed. Firstly, the Internet back-haul and the software algorithms running on low cost hardware must operate rapidly enough to keep up with the wireless link. Secondly, the deluge of information propagating over the back-haul must be maintained to a reasonable level. The second issue is much

¹enet.bespin.org/

²We assume that electromagnetic reciprocity cannot be assumed on such a vast network so that the down-link channels have to be fed back over the wireless link

more pressing since the exponential increase in traffic over the back-haul as one scales from tens to thousands of SNs will eventually prevail even for high speed DSP and fibre-optic back-haul. For now we deal with the first issue.

We employed two computers; each with a dual core 2GHz clock processor connected via three types of link. (i) a direct link, (ii) a switch and (iii) the Internet (ADSL2). The switch and direct links were nominally 100Mbps Ethernet but an SSH secure-copy showed an effective data rate of 85Mbps. The Internet connection was via an ADSL2 link of up-load bandwidth 0.882Mbps and down-load bandwidth 8.03Mbps tested in the same way. A large file of 132kB was used to simulate a beam-forming information packet that would be expected over the wireless network.

TABLE I
P2P BACK-HAUL TRANSMISSION RESULTS

Link	Computer 1 (Mbps)	Computer 2 (Mbps)
direct	11.71	12.47
switch	8.37	8.57
ADSL	2.43	1.33

The results are shown in table I. Not surprisingly, the P2P data exchange runs at a speed lower than and in proportion to the back-haul bandwidth available. There also appears to be a fairly large effect on throughput due to the computers keeping up with the network speed. This effect is much less prominent for the slower ADSL2. Generally speaking the computers exchanged data at a similar rate thus facilitating uniform throughput. These results demonstrate that network speed could be a real issue when designing an SDD-MIMO network.

VI. CODING COMPLEXITY

The large SINR in conjugate match beam-forming requires complex forward error correction processing to handle high bit error rates. Fortunately modern advanced codes can deal with error-rates up to 15-20%. For example Low Density Parity Check Codes can achieve this for rates of $1/2 - 1/4$. Fig. 8 demonstrates some performance examples.

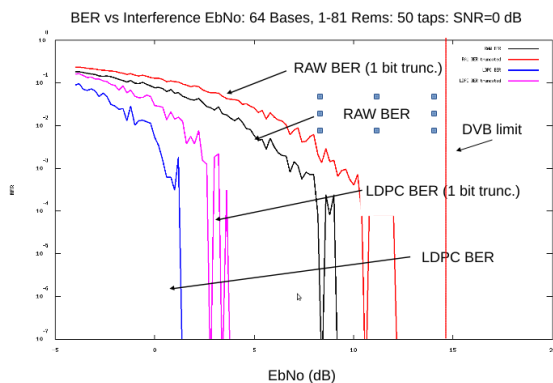


Fig. 8. LDPC performance.

A major challenge for the present project is to implement these codes in low cost hardware [4] where our target is to push LDPC into the regime of 10Mbps information throughput.

VII. CONCLUSION

In this paper we addressed the engineering and physical aspects of SDD-MIMO. We took a mathematical look at how the beam-forming works and how a Monte-Carlo simulation based on a novel correlation definition of capacity leads to some important insights. In particular we discovered that the capacity per user approaches the mean for large SDD-MIMO networks. These insights have contributed to the implementation of the algorithms thus far in ANU-MIMO [4]. We presented experimental results of a simple GPS based synchronisation technique. We investigated the performance of back-haul beamforming over a TCP-IP network. Finally we demonstrated the need for advanced coding to cope with the high SINR in conjugate match beam-forming.

Future issues include the development of a channel codec where forward error correction can operate in the range of 10Mbps on low cost hardware and the implementation of low cost beam-forming algorithms over consumer-grade Internet back-haul networks.

ACKNOWLEDGMENTS

The authors would like to acknowledge the financial support of the Research School of Physics and Engineering at the Australian National University. Gerard Borg would especially like to acknowledge the hospitality of Profs. Teddy Mantoro and Media Ayu.

REFERENCES

- [1] Gerard Borg, Zia-Ud-Din Javaid and Asaduzzaman Khandaker. "SDD-MIMO: Ubiquitous Embedded MIMO for community broadband." . Proceedings of the Fourth International Conference on Computing Engineering and Design, Nusa Putra, Thailand Sep 6-8, 2019.
- [2] Gerard Borg, Zia Ud-Din Javaid, Michael Blacksell, Paul Redman, Daniel Tempra, Marina Artyasa, Teddy Mantoro and Media A. Ayu. "ANU-MIMO: A Community Wireless Network Infrastructure for Remote Populations," . Proceedings of the Fourth International Conference on Computing Engineering and Design, Nusa Putra, Thailand Sep 6-8, 2019.
- [3] H. Yang and T. Marzetta, "Performance of Conjugate and Zero-Forming Beamforming in Large-Scale Antenna Systems," IEEE Journal On Selected Areas in Communications, vol. 31(2) 2013 pp. 172-179.
- [4] G.G. Borg, M. Blacksell, J-C Lonchamp, L. Materne, P. Redman and D. Tempra. "ANU-MIMO: A Decentralised, Scalable and Economical Wireless 5G Building Block for Massive Broadband Connectivity," [http://users.cecs.anu.edu.au/ Gerard.Borg/public/ANU-MIMO_whitepaper.pdf](http://users.cecs.anu.edu.au/Gerard.Borg/public/ANU-MIMO_whitepaper.pdf) [accessed 5-07-2018].
- [5] X. Zhou, J.M. Llorente, A. Adenet, C. Lemasson, P. Kyritsi, and P. Eggers, 2007, "Assessment of MISO Time Reversal for short-range communications in the 5GHz ISM band," in Springer Wireless Personal Communications, 43(2), pp.-759-776
- [6] Mathias Fink. "Time-Reversed Acoustics". Scientific American, November 1999. pp.-91-97.
- [7] James V. Stone. "Information Theory, A tutorial introduction". Sebtel Press, 2015. pp.-162-164.
- [8] R. Barton and R. Zheng, "Order optimal data aggregation in wireless sensor networks using cooperative time-reversal communication," Proceedings of the 40th Annual Conference on Information Sciences and Systems (CISS) and Princeton, NJ, pp. 10501055, 2006.